

Fatigue Life Prediction using Forces in Welded Plates of Moderate Thickness

Pär Fransson
Gert Pettersson

Department of Mechanical Engineering
University of Karlskrona/Ronneby
Karlskrona, Sweden
2000

Thesis submitted for completion of Master of Science in Mechanical Engineering with emphasis on Structural Mechanics at the Department of Mechanical Engineering, University of Karlskrona/Ronneby, Karlskrona, Sweden.

Abstract: A new finite element based method for fatigue life prediction has been examined. The method uses nodal forces and moments along the weld toe to define a structural stress perpendicular to the weld. The method was found to be less mesh-sensitive than ordinary post-processing.

Keywords:

Fatigue Life Prediction, Fillet Weld, Weld toe, Finite Element Method, Shell elements, Nominal Stress, Structural Stress,

Acknowledgements

This work was carried out at the Department of Mechanical Engineering, University of Karlskrona/Ronneby, Karlskrona, Sweden, under the supervision of Dr. Mats Walter.

The work was initiated in 1999 as a co-operation between Volvo Articulated Haulers AB and the Department of Mechanical Engineering at the University of Karlskrona/Ronneby.

We wish to express our gratitude to Dr. Mats Walter and Dr. Göran Broman, University of Karlskrona/Ronneby, and M.Sc. Bertil Jonsson, Volvo Articulated Haulers AB, for their scientific guidance and support throughout the work.

We also like to thank Dr. Mikael Fermér Volvo Car Corporation for rewarding discussions, and Volvo Construction Equipment Components AB for their help with the experimental part of this work.

Finally, we would like to thank our colleagues in the Master of Science programme and all the other members of the Department of Mechanical Engineering for valuable discussions and support.

Karlskrona, January 2000

Pär Fransson

Gert Pettersson

Contents

1	Notation	5
2	Introduction	7
3	Conventional Stress Determination	8
3.1	Theory	8
3.1.1	Nominal Stress Approach	8
3.1.2	Hot Spot Stress Approach	9
3.1.3	Local Notch Stress Approach	10
3.1.4	Fracture Mechanism	10
4	The Volvo Approach	11
4.1	Basic Idea	11
4.2	Calculation of Structural Stress	12
4.2.1	Global vs. Element Co-ordinate System	13
4.2.2	Start/end and Sharp Corners of Welds	13
4.2.3	Smooth Corners and Lines	15
4.3	Different Ways of Modelling Corners	15
4.4	Effect of Element Size	17
4.5	Meshing Rules	21
5	Fatigue Resistance	22
5.1	Basic Principles	22
5.2	Fatigue Resistance of Classified Structural Details	23
6	FE-models	24
6.1	FAT 511	24
6.2	FAT 521	26
6.3	FAT 523	27
6.3	Volvo Case	28
7	Experimental Results	29
7.1	Test Object	29
7.2	Weld Class	30
7.3	Experimental Set-up	31
7.4	Results	33
7.5	Hot-Spot Stress	35
8	Computer Program	37
8.1	Input	37

8.2 Program Logic	37
8.3 Output/Calculated Result	39
9 Conclusions	40
10 Further Work	42
11 References	43

1 Notation

A	Area	[m ²]
E	Young's modulus	[Pa]
F	Force	[N]
I	Area moment of inertia	[m ⁴]
K	Stiffness	[N/m]
M	Moment	[Nm]
N	Number of cycles	[-]
R	Stress ratio	[-]
S	Stress amplitude	[Pa]
T	Force	[N]
W	Flexural resistance	[m ³]
Q	Force	[N]
g	Node	[-]
k	Slope	[-]
m	Line moment	[Nm/m]
n	Line force	[N/m]
q	Line force	[N/m]
σ	Stress	[Pa]
ε	Strain	[-]
ν	Poisson's ratio	[-]

Indices

a	Attachment
b	Bending
p	Plate
s	sseeked
<i>E</i>	Element
max	Maximum
min	Minimum
nom	Nominal
hs	Hot spot
x, y, z	Directions
⊥	Perpendicular
[]	Matrix

2 Introduction

In heavy contract vehicles, e.g. haulers and wheel loaders, the fatigue life prediction is often the dominating design case. In order to optimise the welds and the geometry according to quality and weight a development of the existing calculation methods is desirable. A new method, which is going to be examined in this thesis, starts with a FE-model, using shell elements, including the welds and continues, collecting nodal forces and nodal moments from which the structural stress in the interesting point, e.g. the weld toe, is calculated. Stresses calculated from nodal forces and moments have the advantage of not being so sensitive to element size as normal calculated element stresses. This approach also makes it possible to separate the contributions from bending moment and nodal force on structural stress. This method was first proposed and presented in 1995 by Fayard J-L., Bignonnet A. and Dang Van K. [1] In this approach, however, the weld was modelled with beam elements. In 1997 Magnus Andréasson and Björn Frodin performed a master thesis [2] at Volvo Car Corporation, VCC, in which shell elements were used on thin plates. The aim with this master thesis is to examine the possibility to apply the method on moderate plate structures such as e.g. a hauler frame and to develop a MATLAB code which is able to read data from a FE-program and calculate the desirable stresses. The work has been performed for Volvo Articulated Haulers AB, Växjö, Sweden, in co-operation with Department of Mechanical Engineering, University of Karlskrona/Ronneby.

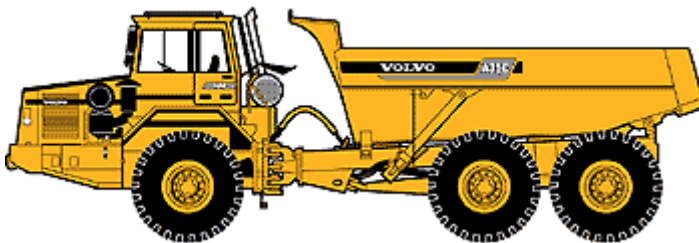


Figure 2.1. Articulated Hauler, Volvo A35C.

3 Conventional Stress Determination

3.1 Theory

The actual stress state in a weld is difficult to determine depending on, among others, variations in the weld profile, haphazard defects in the weld, residual stresses in the structure etc. These different factors make fatigue resistance difficult to predict. There are today four basic approaches to fatigue life prediction of welded components:

- the nominal stress approach;
- the hot spot stress approach;
- the local notch stress approach;
- the fracture mechanics approach.

This section aims at giving a short overview of the different approaches.

3.1.1 Nominal Stress Approach

In this approach [5,7] the fatigue resistance is determined by practical tests which are performed on either small testpieces or in full scale. The testpieces are equipped with different types of attachments and varying weld-types, which causes stress-raising effects. When fatigue at the welded attachment is considered, the nominal stress is calculated in the region containing the weld detail but excluding any influence of other attachments on the stress distribution. Thus, all structural discontinuity effects and local notch effects are included in the fatigue strength so determined. Nominal stress is calculated according to the basic formula:

$$\sigma_{nom} = \frac{F}{A} + \frac{M}{W_b} \quad (3.1)$$

The nominal fatigue strength for several different types of attachments are specified. The fatigue strength is presented in the form of S-N curves, also named Wöhlerdiagram.

3.1.2 Hot Spot Stress Approach

In this approach [5,7-9] the fatigue strength is based on strain measurements in association to the expected fractured zone, in this case the weld toe. The measurement is made on specified distances from the critical point (the hot spot), figure 3.1.

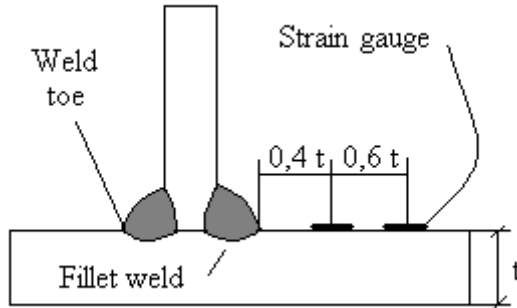


Figure 3.1. Measuring hot spot stress with strain gauges.

Usually two strain gauges with two perpendicular measuring grids are used in order to take the stress biaxiality into account. Assuming that the shear strain near the weld is negligible the stress perpendicular to the weld can be calculated according to equation 3.2.

$$\sigma_{hs} = E \varepsilon_x \cdot \frac{1 + \nu \frac{\varepsilon_y}{\varepsilon_x}}{1 - \nu^2} \quad (3.2)$$

The hot spot stress is then extrapolated from the two points towards the weld toe. Unlike the nominal method, the hot spot approach is not dependent on which type of attachment being analysed. This reduces the number of S-N curves considerably.

3.1.3 Local Notch Stress Approach

This approach [5,7] is based on the stress state at the notch directly. All stress raisers must therefore be taken into account in the analyse. The analyse will often be divided into a global FE analyse at the structural level combined with a local analyse at the notch area. To take account of all the variations in weld profile, an effective notch radius of 1 mm replaces the real contour, figure 3.2.

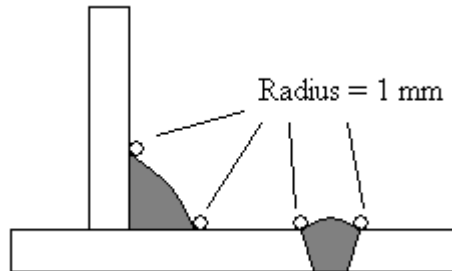


Figure 3.2 Effective notch radius.

The method is restricted to welded joints, which are expected to fail from the weld toe or root. Other causes of fatigue failure are not covered. The approach is not suitable if there are considerable stress components present parallel to the weld.

3.1.4 Fracture Mechanism

In this approach [5,7,10], stress analysis is used to determine the value of the stress intensity factor range which, besides stresses, depends on the crack length and the geometry around the crack. For weld toe fatigue cracks, the effect of the local notch decreases, as the crack becomes deeper. Fracture mechanism has a large potential for analysing most of the phenomenon's present at a weld. Its disadvantage is however that it is time consuming to perform.

4 The Volvo Approach

This chapter aims to give a detailed account of the approach that underlies this thesis. The proposed method was introduced in 1995 by Fayard, Bignonnet and Dang Van [1]. The method has also been tested on welded thin sheet structures in a master thesis from Chalmers University of Technology [2].

The general procedure is outlined in Section 4.2 after which a number of particular cases are discussed in the following subsections, 4.2.1–4.2.3. Different ways of modelling corners have been tested, which is discussed in Section 4.3. Further, in Section 4.4, a comparison is made between stresses calculated by I-DEAS and stresses, here called structural stresses, calculated with the proposed method. Finally, in Section 4.5 a number of meshing rules are given.

4.1 Basic Idea

Fatigue cracks can occur in different locations in a fillet weld. In this approach the cracks are assumed to occur parallel with the weld toe. For that reason the structural stress is defined as the stress perpendicular to the weld toe, σ_{\perp} . This stress is caused by the force perpendicular to the weld and of the moment parallel with the weld according to equation 3.1. The necessary forces and moments are calculated by the FE-solver directly from the nodal displacements and rotations according to equation 4.1. These forces and moments are in I-DEAS denominated “Element forces”.

$$[F_E] = [K_E] \cdot [u_E] \quad (4.1)$$

When making a FE-model of a sharp corner the stress in this corner, theoretically, raises towards infinity. In practice stresses are dependent on both the size and the quality of the mesh. Stresses calculated using equation 3.1, with forces and moments from 4.1, are, however, not in the same way dependent on the mesh. In this way a FE-based calculation method, comparatively independent on the mesh size, can be created.

4.2 Calculation of Structural Stress

The structural stress consists of two components, the normal stress derived from the force, N_x , perpendicular to the weld-line ($g_1 - g_2$), and a bending stress derived from the moment, M_y , parallel to the weld-line, figure 4.1. The nodal forces, e.g. N_{x1}^1 acting on node g_1 in figure 4.1, shall be considered as external forces acting on the element. Thus, the force is a pressure force.

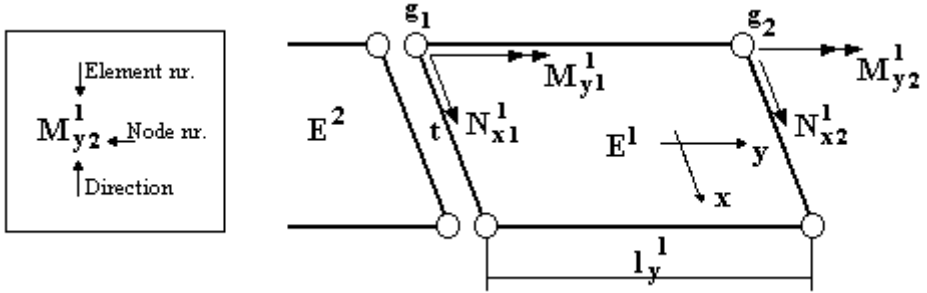


Figure 4.1. Shell element with nodal force and moment.

Transferring these nodal forces and moments into a line moment, m_y , and a line force, n_x , the structural stress in element E^1 can be calculated as [3]:

$$\sigma_{\perp}(y) = -\frac{n_x(y)}{t} - \frac{12 \cdot m_y(y) \cdot z}{t^3} \quad (4.2)$$

where z is the distance from the mean surface in the z -direction. Calculated nodal forces and moments have to be transformed into line forces and line moments. Each element generates two boundary values located at $y=0$ and $y=l_y^1$. The values for these points can be written as [4]:

$$m_y^1(0) = \frac{2}{l_y^1} (2 \cdot M_{y1}^1 - M_{y2}^1) \quad (4.3)$$

$$m_y^1(l_y^1) = \frac{2}{l_y^1} (2 \cdot M_{y2}^1 - M_{y1}^1) \quad (4.4)$$

$$n_x^1(0) = \frac{2}{l_y^1} (2 \cdot N_{x1}^1 - N_{x2}^1) \quad (4.5)$$

$$n_x^1(l_y^1) = \frac{2}{l_y^1} (2 \cdot N_{x2}^1 - N_{x1}^1) \quad (4.6)$$

The structural stress at the top surface, $z=t/2$, can then be calculated at the two grid-points g_1 and g_2 by substituting equation 4.3 – 4.6 into equation 4.2 which gives the final expressions, assuming $\sigma_{\perp}(0)=\sigma_{\perp}(g_1)$ and $\sigma_{\perp}(t_y)=\sigma_{\perp}(g_2)$, according to:

$$\sigma_{\perp}(g_1) = -\frac{2(2 \cdot N_{x1}^1 - N_{x2}^1)}{l_y^1 \cdot t} - \frac{12(2 \cdot M_{y1}^1 - M_{y2}^1)}{l_y^1 \cdot t^2} \quad (4.7)$$

$$\sigma_{\perp}(g_2) = -\frac{2(2 \cdot N_{x2}^1 - N_{x1}^1)}{l_y^1 \cdot t} - \frac{12(2 \cdot M_{y2}^1 - M_{y1}^1)}{l_y^1 \cdot t^2} \quad (4.8)$$

4.2.1 Global vs. Element Co-ordinate System

In the initial phase of the project there was a discussion whether it was the global co-ordinate system or the local element co-ordinate system that should be used. After some investigations it turned out that forces and moments presented by I-DEAS in “Element forces” are related to the global co-ordinate system. The choice of co-ordinate system is, in principle, of no significance except when programming the MATLAB code for stress calculations.

4.2.2 Start/end and Sharp Corners of Welds

Starts/stops as well as corners and other geometrical change causes stress concentrations. The line of action when modelling these points follows the same approach as in the master thesis from Chalmers [2]. Starts and ends are modelled according to figure 4.2 (a) and sharp corners according to 4.2 (b). With the method proposed, no extra refinement is needed at these points. In these cases four different stresses, $\sigma_{\perp 1} - \sigma_{\perp 4}$, could be calculated for a single node, equation 4.9 – 4.12 and figure 4.3. Note that in element E_2 the structural stress are calculated in two different directions parallel to the element sides. The structural stress σ_{\perp} is, as before, assumed to be the maximum magnitude, with maintained sign for the node.

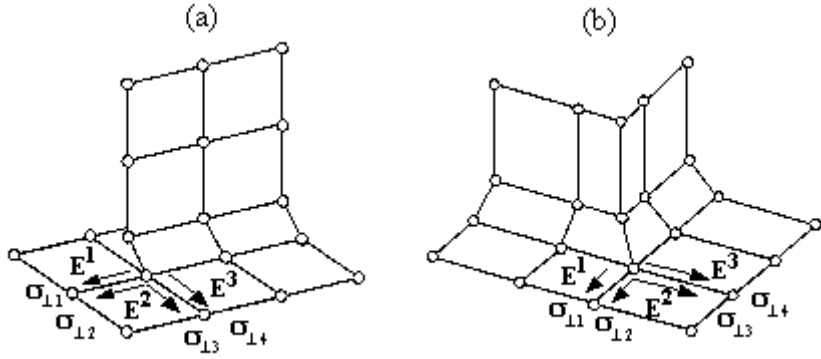


Figure 4.2. Start/end of weld (a) and sharp corner (b).

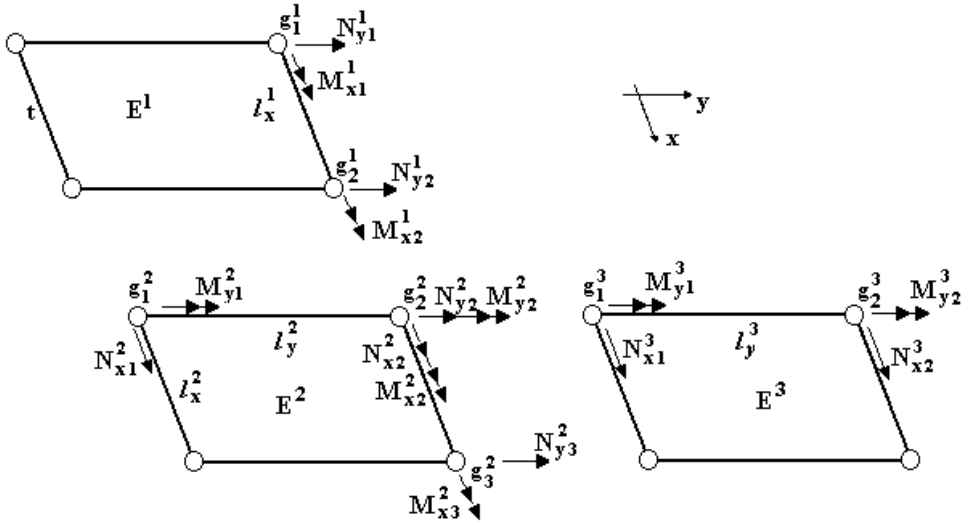


Figure 4.3. Forces, moments and element lengths used in structural stress calculation..

$$\sigma_{11} = \frac{2 \cdot (2 \cdot N_{y2}^1 - N_{y1}^1)}{l_x^1 \cdot t} - \frac{12 \cdot (2 \cdot M_{x2}^1 - M_{x1}^1)}{l_x^1 \cdot t^2} \quad (4.9)$$

$$\sigma_{12} = \frac{2 \cdot (2 \cdot N_{y2}^2 - N_{y3}^2)}{l_x^2 \cdot t} - \frac{12 \cdot (2 \cdot M_{x2}^2 - M_{x3}^2)}{l_x^2 \cdot t^2} \quad (4.10)$$

$$\sigma_{\perp 3} = -\frac{2 \cdot (2 \cdot N_{x2}^2 - N_{x1}^2)}{l_y^2 \cdot t} - \frac{12 \cdot (2 \cdot M_{y2}^2 - M_{y1}^2)}{l_y^2 \cdot t^2} \quad (4.11)$$

$$\sigma_{\perp 4} = -\frac{2 \cdot (2 \cdot N_{x1}^3 - N_{x2}^3)}{l_y^3 \cdot t} - \frac{12 \cdot (2 \cdot M_{y1}^3 - M_{y2}^3)}{l_y^3 \cdot t^2} \quad (4.12)$$

4.2.3 Smooth Corners and Lines

In practice, it's not common that a weld line exactly follows a global coordinate direction. In these cases FE calculated forces and moments are not longer perpendicular respective parallel to the weld line. The resulting forces and moments must however be transformed to directions perpendicular and parallel to the weld line. This is done using common trigonometry. The structural stress can then be calculated according to equation 4.9 and 4.10. When calculating the structural stress along a weld line, only elements with one side in common with the weld are taken into consideration.

4.3 Different Ways of Modelling Corners

It is not obvious how to model a smooth corner. Different ways of building the FE-model results in varying stresses. Three different ways of modelling the corner have been tested. The appearance of the models and the structural stress they cause are shown in figure 4.4 – 4.6. FAT 521, figure 6.3 (the different models will be described more detailed in Chapter 5), has been used as basic data in the test. The model has been loaded with a nominal tensile stress of 100 MPa. On the basis of the received results, the best way of creating a smooth corner seems to be according to figure 4.6. This method is used further on.

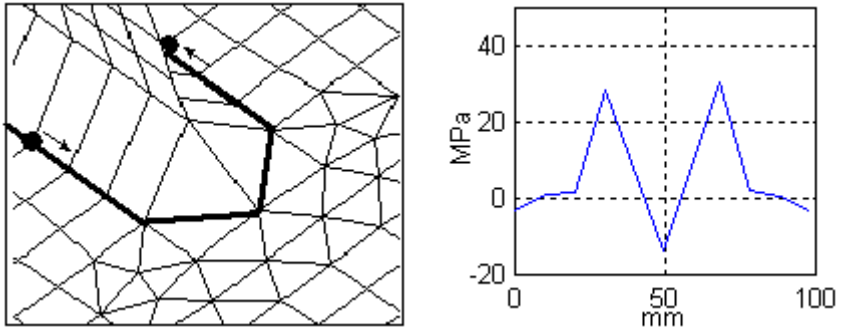


Figure 4.4. Corner and stress distribution.

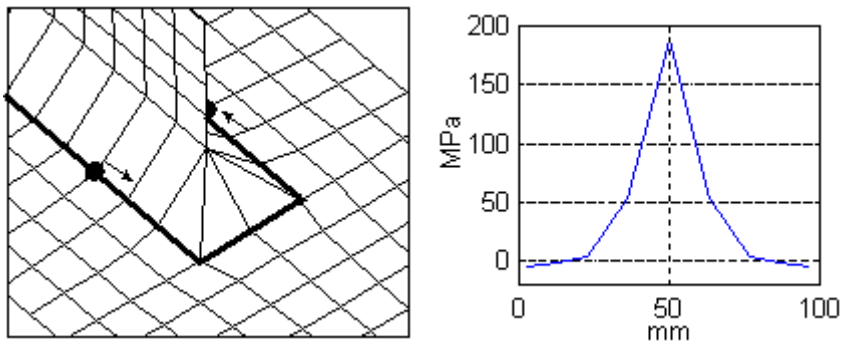


Figure 4.5. Corner and stress distribution.

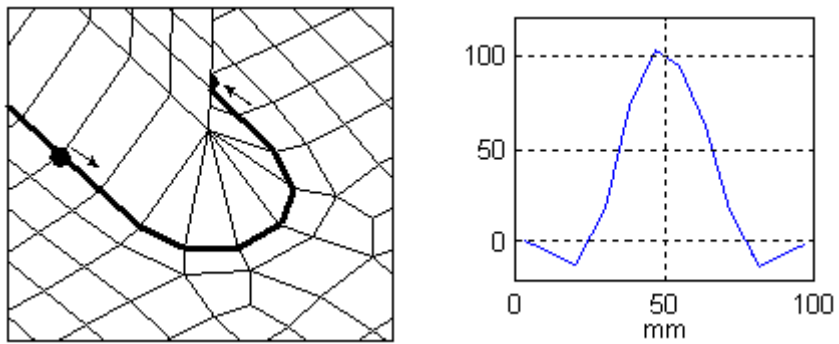


Figure 4.6. Corner and stress distribution.

4.4 Effect of Element Size

One of the main thesis in the proposed method, that the calculated stresses should be less mesh dependent than stresses calculated by a “ordinary” FE-solver has been tested on case FAT 521, figure 4.7 a-d. The geometry of the part includes corners where stress concentrations and local deformation appear. Four different grids were used in the comparison. In every case the model were loaded with a 100 MPa tensile stress.

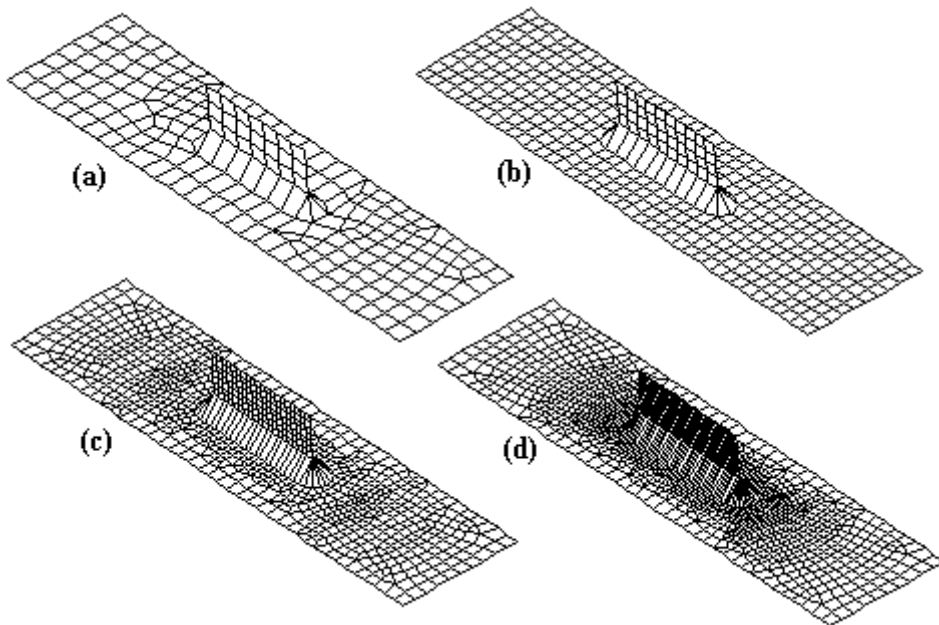


Figure 4.7. Different mesh. (a) 15mm (b) 10mm (c) 5mm (d) 2.5mm.

The structural stress along the weld line was calculated according to the approached method. The received results were expected to be some type of smooth curves but instead they showed high irregularity, figure 4.8. This behaviour were not expected and caused quit a lot of problems. It turned out that Dr. Mikael Fermér, Volvo Car Corporation [2] had run into the same problem. The problem were, in his case, caused by the fact that GPFORCE in NASTRAN included both normal and shear forces acting on the nodes. Averaging the two nodal-values, which eliminated the influence of the shear forces, would solve the problem. The result of averaging the results

achieved by the Volvo method indicated that the Element Forces in the IDEAS Universal File probably also included the shear forces, figure 4.9. Since the IDEAS Universal File were the only way to get results out of IDEAS, unlike NASTRAN which had several other opportunities, averaging were decided to be used further on despite the fact that this cause another problem. When the weld is not closed, the results in the end-nodes can not be averaged.

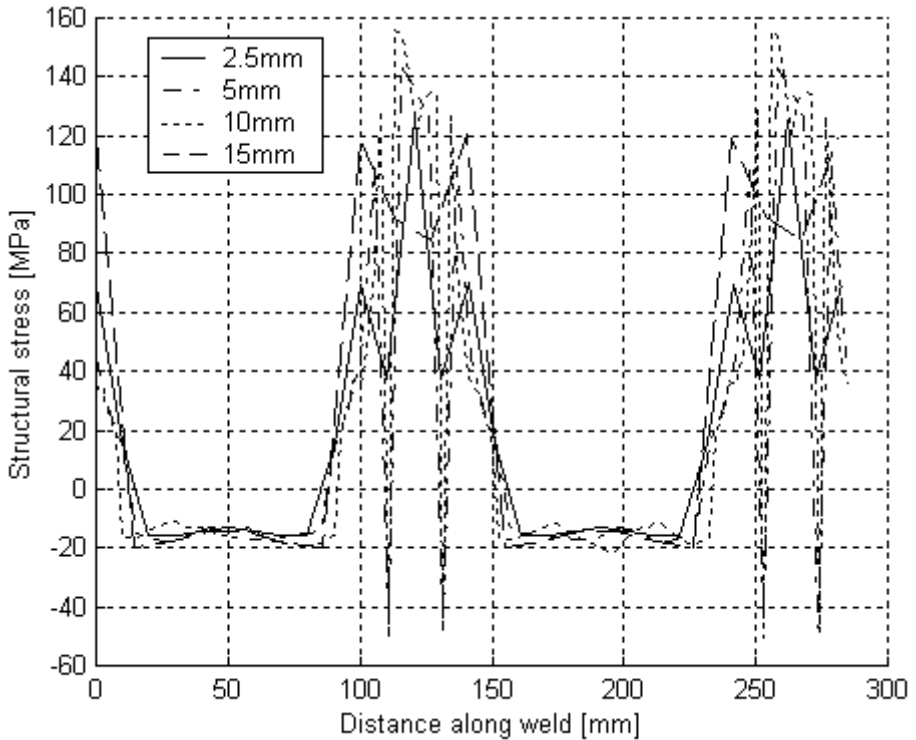


Figure 4.8. Structural stress, Volvo approach.

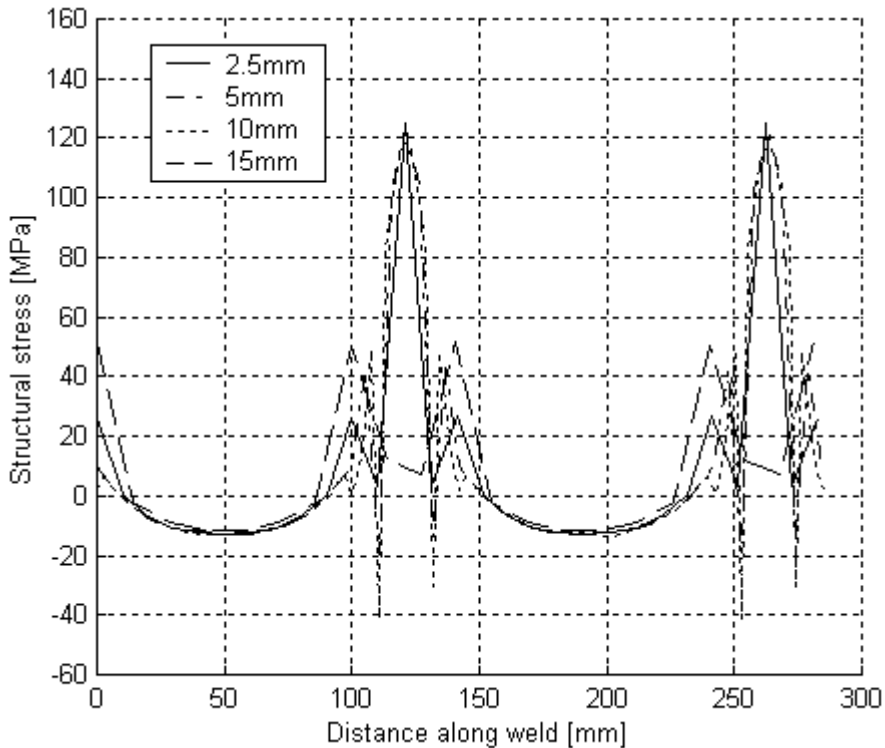


Figure 4.9. Structural stress, Volvo approach. Mean value.

The curves were now smoother than before but still, there were irregularities. This could be explained by the fact that some elements only have one node, out of four, located at the weld line, red marked in figure 4.10 a, and that they causes disturbance in the force field. These elements could, according to the original approach, not be considered in the calculations since they do not have an element length along the weld toe. Unfortunately it showed that it was not convenient to use free mesh. To avoid this problem, the area around the weld toe should be mapped meshed, figure 4.10 b.

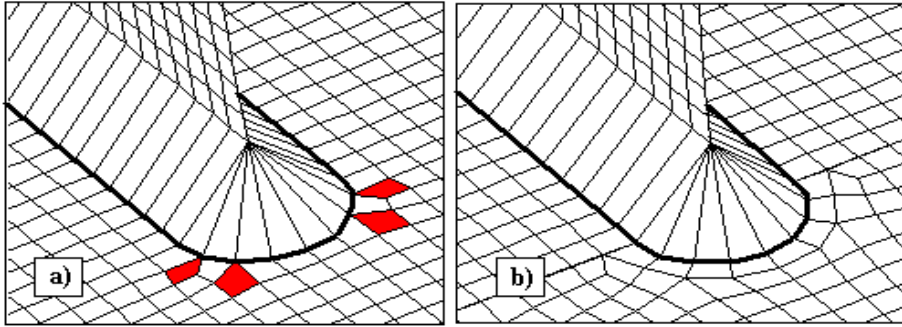


Figure 4.10. Free mesh,(a), around a corner, and the same corner but this time with a mapped meshed (b).

Finally the stresses calculated by I-DEAS, figure 4.11, were compared with the results achieved by the proposed method. As assumed, the Volvo approach showed a less mesh dependent behaviour. When using the Volvo approach the stress raises 6 % while decreasing the mesh-size from 10 to 2.5 mm. This should be compared with 26 % while doing the same in I-DEAS. The 15-mm mesh is excluded from the comparisons because of too much influence from distorted elements around the weld.

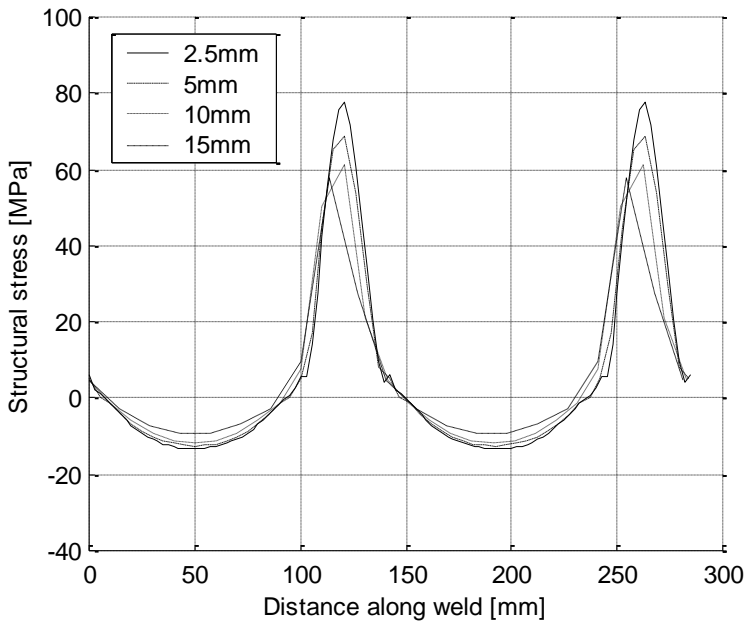


Figure 4.11. Structural stress, I-DEAS

4.5 Meshing Rules

The proposed method calls for some meshing rules.

- The structure should be meshed with four node shell elements. The thickness of the elements should be constant.
- The weld should also be meshed with four node shell elements except in smooth corners where three node shell elements can be used. The element thickness should be the same as the effective throat, figure 4.12.
- The plates are described by their mean surfaces.
- The nodes of the elements representing the weld are positioned $t/2$ below the toes, figure 4.12.
- To straighten up the mesh near e.g. a smooth corner, partition or anchor nodes can be used.
- Sharp element corners are not allowed up to the weld toe. The elements must have a surface towards the weld toe, figure 4.10 b.

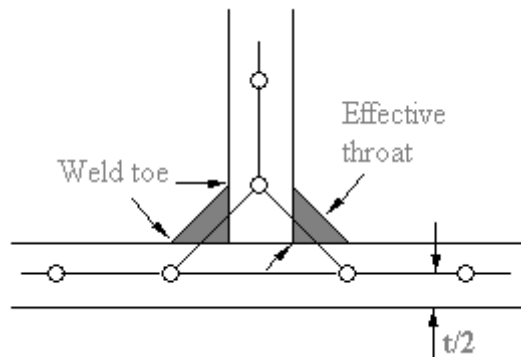


Figure 4.12. Cross-section of weld connection between two thin shells.

5 Fatigue Resistance

Material, exposed for varying loads, can break even if the load level is far below the yield limit. This chapter aims to refresh the most elementary parts of the mechanics of materials concerning fatigue. In Chapter 5.1 some common conceptions are defined, which are used in this thesis. Chapter 5.2 concerns some basic facts about the models used in this work.

5.1 Basic Principles

A fatigue fracture process can be divided into three phases. The first phase is the so-called crack formation phase. When a crack have been initiated, crack growth occurs. When the crack has become sufficiently big, fatigue fracture occurs.

When determine fatigue data for a structure, test details are loaded with a cyclically varying force. The variation can be either of constant amplitude (CA) or more common of type spectrum. The CA-type can best be described using the three numbers σ_{\max} , σ_{\min} and R, equation 5.1.

$$R = \frac{\sigma_{\min}}{\sigma_{\max}} \tag{5.1}$$

Often used cases are pulsating loads where $R=0$ and alternating loads where $R=-1$, see figure 5.1. The spectrum load types, which are dominating for vehicles, have a variation, which is not easily described. One way is to use the so-called rainflow method, which results in a diagram over cycles at different load levels.

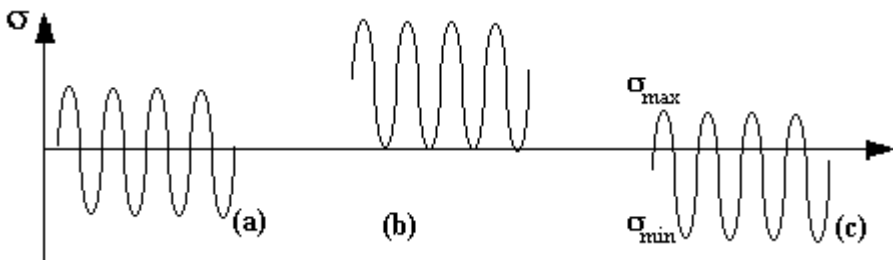


Figure 5.1. Alternating load (a), pulsating load (b) and varying load (c).

The results from fatigue tests are often compiled into a S-N diagram, also called Wöhlerdiagram, where the logarithm of the stress amplitude is plotted as function of the logarithm of the number of cycles to fracture (log-log). Also log-lin diagram is used. In a certain interval there is in a log-log-diagram a, more or less, linear relation between stress amplitude and cycles to failure. With a known endurance, N , at a known stress-level, σ , and a known slope of the endurance curve it's possible to calculate the endurance, N_s , at other stress levels, σ_s , or vice versa. For welds the slope $k=3$ is often used. The relationship between the terms can be described according to [6]:

$$\left(\frac{\sigma}{\sigma_s}\right)^k \cdot N = N_s \quad (5.2)$$

A Wöhlerdiagram is, unless otherwise stated, constructed so that the curve corresponds to a 50 % fracture probability.

5.2 Fatigue Resistance of Classified Structural Details

The fatigue assessment of classified structural details and welded joints, used in this thesis, is based on the nominal stress range. All fatigue resistance data [5] are assumed to have a survival probability of at least 95 % unless otherwise stated. The fatigue curves, used in Chapter 6, are based on representative experimental investigations and includes the effect of e.g. structural and local stress concentrations, variations in the weld profile and welding residual stresses. Each fatigue strength curve is identified by the characteristic fatigue strength of the detail at 2 million cycles. This value is the fatigue class (FAT). The slope of the fatigue strength curves assessed on the basis of normal stresses is $k=3$.

6 FE-models

One of the purposes with this master thesis was to compare stresses calculated with the proposed method with known fatigue data. Nominal stress can, using a FE-solver and the proposed method, be recalculated to stresses in the weld toe. Known FAT-values can be recalculated according to equation 5.2. All FAT values are given for $2 \cdot 10^6$ cycles. In Chapter 6.1-6.3, three standardised types of attachments from the 500-serie [5] are examined. In chapter 6.4 a special Volvo designed attachment is examined. In this case, which also underlies the experimental part of this thesis there is no known data.

6.1 FAT 511

The FAT511 is a transverse attachment, which should not be thicker than the main plate. The dimensions of the plate used in this simulation is 100 x 200 mm and the height of the attachment is 50 mm. Figure 6.1 a-c shows how loads and boundary conditions are applied. The FAT value for this attachment is 100 MPa. Three different load cases have been tested. Apart from the FAT-value, FE-calculations have also been made for nominal loads of 75 and 50 MPa. The results from these calculations are shown in figure 6.2.

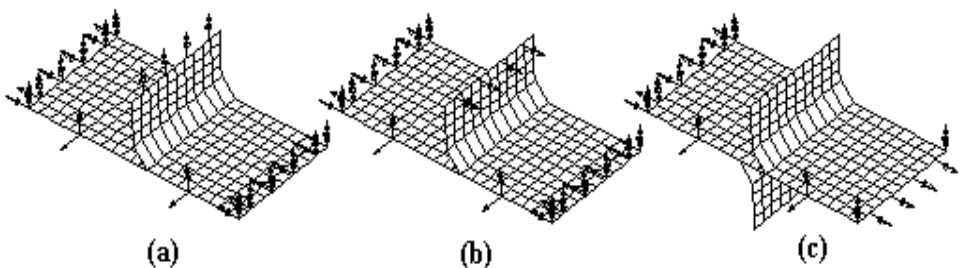


Figure 6.1. FE-models.

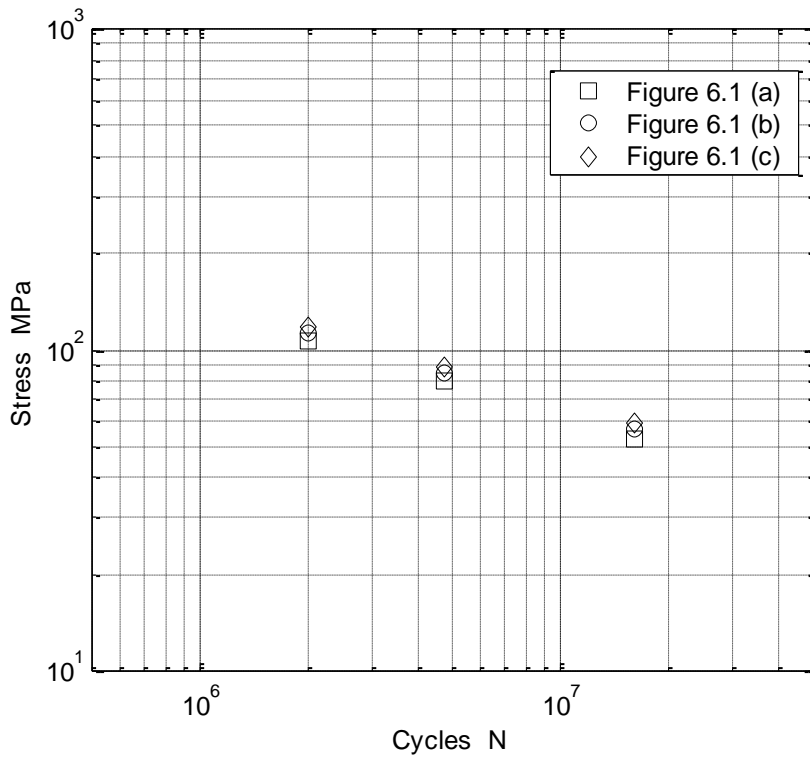


Figure 6.2. Results FAT 511.

6.2 FAT 521

The FAT521 is a longitudinal gusset with varying length. In this case there are different FAT-values for different attachment lengths.

The height of the attachment is 50 mm. The dimensions of the plate used in this simulation is $100 \times l_p$ mm where l_p is the length of the plate according to:

$$l_p = l_a \cdot 2 + 200 \quad (6.1)$$

Figure 6.3 a-b shows how loads and boundary conditions are applied for bending respective tensile stress. The results from the calculations are shown in figure 6.4 and 6.5. Nominal stress is 100 MPa.

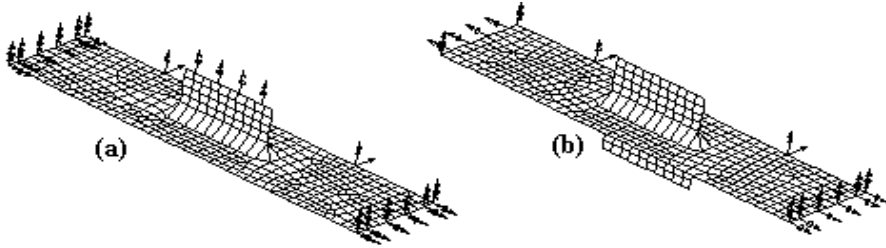


Figure 6.3. FE models.

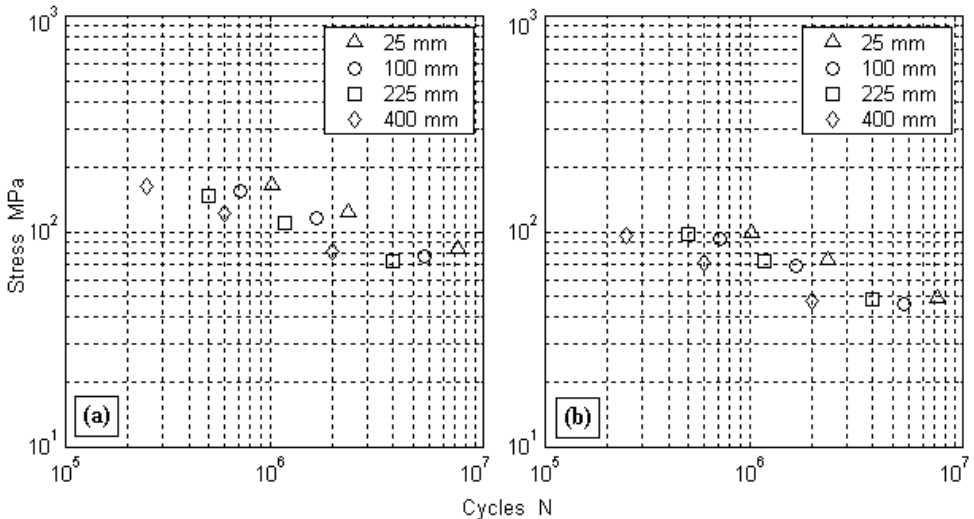


Figure 6.4. Results FAT 521. Bending stress (a) and tensile stress (b).

6.3 FAT 523

The FAT523 is, in the same way as FAT521, a longitudinal gusset. The difference is that the gusset has a smooth transition, which is either sniped or has a radius. The attachment is located on a beam with 100-mm width and 200 mm height. The FAT-value varies depending on the relationship between the transition and the height of the beam. Figure 6.6 a shows the beam. Since there are no data about the length of the attachment all models has been made with an "active attachment area" of 50 x 50 mm, figure 6.6 b. The total length is then depending on the transition. FE-calculations have been made for nominal loads of 100 MPa. The results from these calculations are shown in figure 6.7.

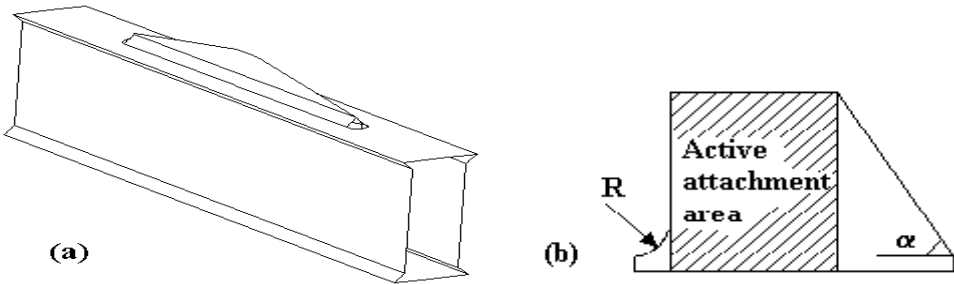


Figure 6.6. FE model.

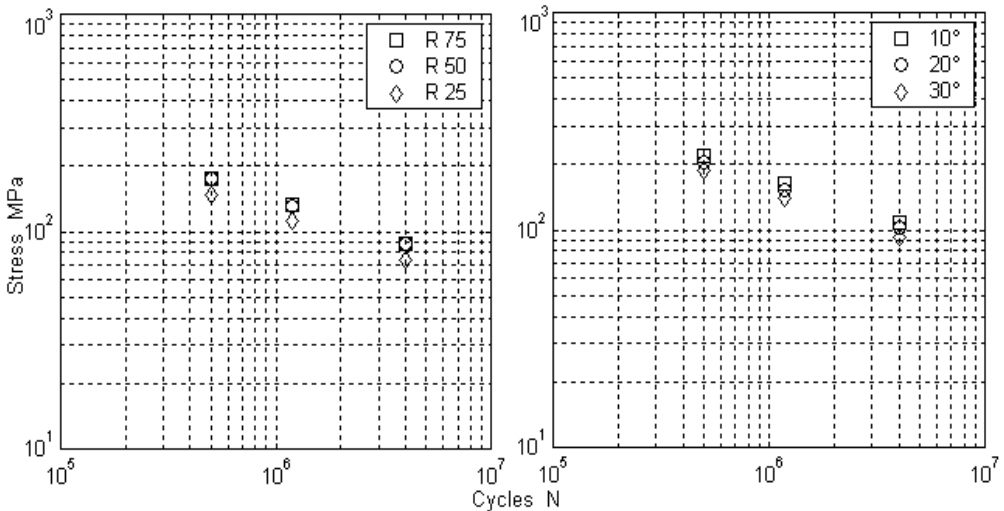


Figure 6.7. Results FAT 523.

6.3 Volvo Case

This attachment shows several similarities with the FAT523. The model is made with three different lengths of the attachment in the same model, figure 6.8, and the dimensions are shown in figure 6.9. The height of the attachment is 50 mm. The dimensions of the beam are the same as in Chapter 6.3. In this case there are no standardised FAT-values for the attachment. Since no FAT-values are available for this attachment the structural stress calculated could not be compared with any known fatigue data. Tests were therefore performed, see Chapter 7. A more detailed description of the beam is given in Chapter 7.

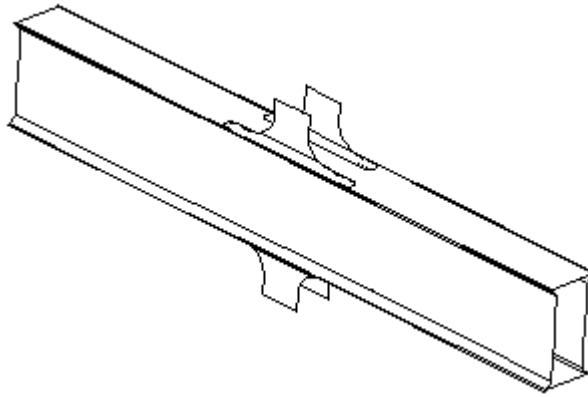


Figure 6.8. Beam with four attachments used in experiment.

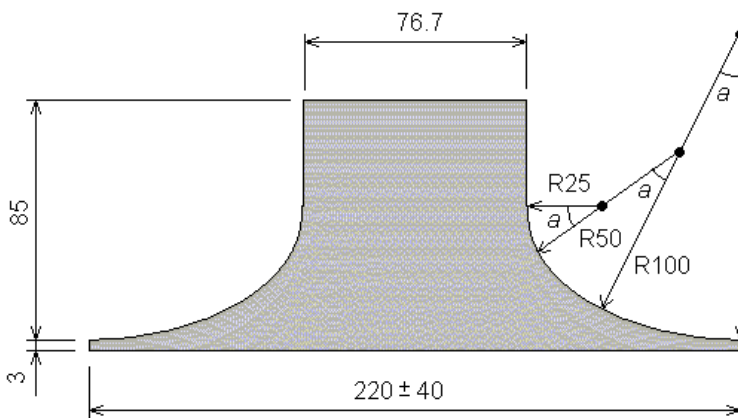


Figure 6.9. Attachment, $a=30^\circ$.

7 Experimental Results

Three beams with four attachments each were specially designed and fatigue tested within this thesis. The shape of the attachment was varied to see if this could have any effect of the fatigue life. A total of twenty-four weld-ends could in this way be tested. The beams were manufactured at Volvo Articulated Haulers AB factory in Braås. The experimental procedure took place in Eskilstuna at Volvo Construction Equipment Component AB.

7.1 Test Object

The objects, which were tested, consist of a beam with four attachments. The beams were manufactured in the shape of a square-profile, figure 7.1, and the attachments according to figure 6.8. The attachment weld were, from both sides, run “into nowhere” to achieve a smooth weld-end. A more detailed description of the beams, with material and weld data, is given in table 7.1.

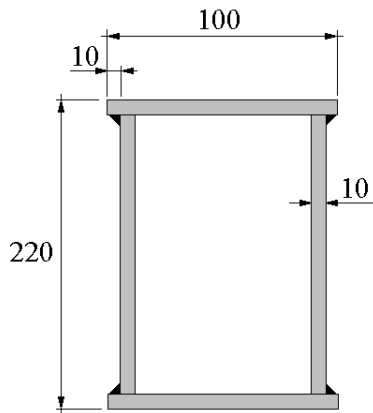


Figure 7.1. Cross section of the beam.

Table 7.1. Beam specification.

<i>Material</i>	Domex 350, $E=210\,000\text{ N/mm}^2$, $\nu=0.3$
<i>Thickness</i>	10 mm in all parts
<i>Weld</i>	Fillet weld, without preparations, throat $a=6$
<i>Length</i>	approx. 2000 mm
<i>Cross section</i>	200x100 mm

7.2 Weld Class

The weld class is a way to describe the weld quality and indicates how well the weld is manufactured, and thereby how resistant it is to fatigue. The quality of the welds on the beam are according to Volvo Corporate Standard STD5605,51 weld class C, which is the weld class with the second lowest requirements. This gives a K_x (stress concentration factor for welds) value of 3,0 [12]. The weld class is C because of surface pores and uneven weld.



Figure 7.2. Two attachments welded on the beam used in experiment. Note how the weld is uneven and the dark dots on the weld.

7.3 Experimental Set-up

The beams in the test have been simply supported. The moment-loss support consists of two small pieces of a HE300 profile. The waist of the two HE300 profiles were used to take care of the angular displacement while the lower flange were clamped against the floor. On the upper flanges of the HE300 profiles, supports were assembled. Into these supports the beam, finally, were mounted, figure 7.3.



Figure 7.3. Simply supported beam.

The load was applied as close as possible to the attachments. The exact positions varied between the beams because of different weld lengths. All dimensions are therefore presented in table 7.2 together with the loading force and the calculated, normal, bending stress. The stresses which are presented are nominal bending stress (amplitude) in point A and B. When calculating these stresses a area moment of inertia of $533.67 \cdot 10^5 \text{ mm}^4$ were used. The frequency varied between 5 and 8 Hz and the stress ratio, R, were -1.

A hydraulic actuator with built in LVDT transducer was used to apply the force to the beam. Between the hydraulic actuator and the beam there were a force transducer, Load Indicator AB Sweden Type 5-178, measuring-range 100 kN, measuring the force and a specially designed attachment which were able to handle possible uneven load. The tests were performed, and load controlled, by an Alltest Industrial Computer 610 Advantech from BIT Scandinavia AB. The experimental set-up is shown in figure 7.4.

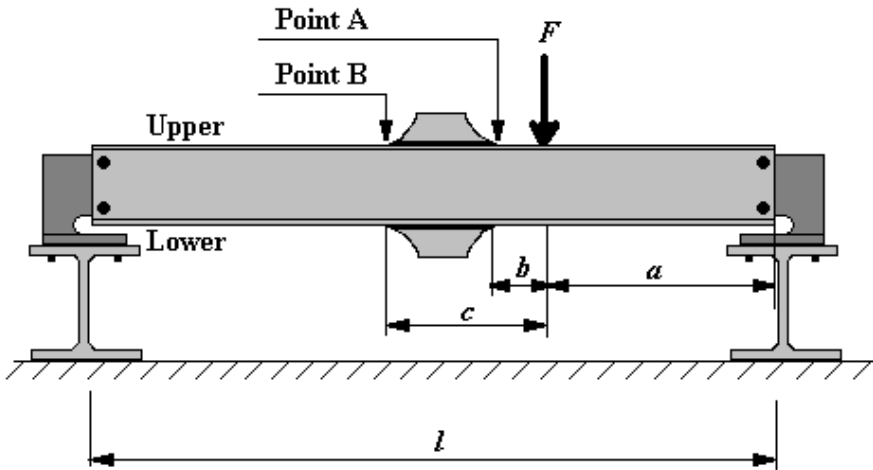


Figure 7.4. Dimensions, measuring-points and loads.

Table 7.2. Dimensions, forces and stresses.

Beam nr.	Upper/ Lower	F	l	a	b	c	Nom. stress range pt. A	Nom. stress range pt. B
		kN	mm	mm	mm	mm	MPa	MPa
1	U	45	2090	835	110	320	154,2	126,0
1	L		2090	835	110	320	154,2	126,0
2	U	48	2120	860	80	320	168,6	134,4
2	L		2120	860	57	337	172,0	132,0
3	U	48	2192	860	85	325	172,4	139,2
3	L		2192	860	62	342	175,6	136,8

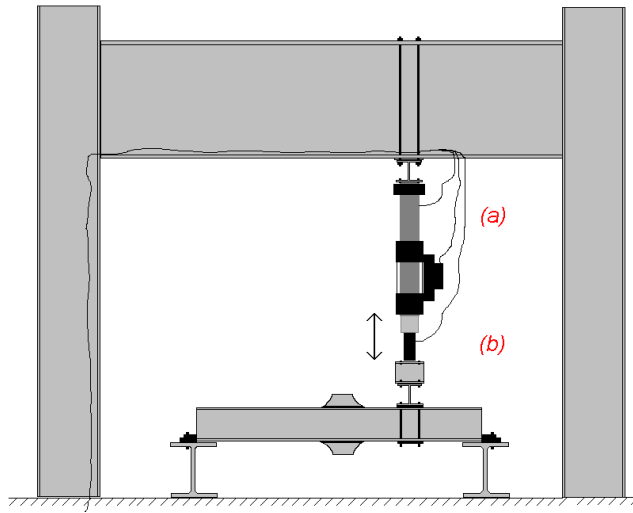


Figure 7.5. Experimental set-up. A hydraulic actuator with built-in LVDT transducer (a) and a force transducer (b).

The deflection of the beam were calculated to 1 mm, but in reality it deflected some more due to low stiffness in the flange of the HE300 profiles. This means that the moment of force was not zero in the support. The moment loss was calculated to 115 Nm in the left HE300 profile and 119 Nm in the right [11]. Since the loss was so small, less than 0,5 %, the influence of this moment loss were neglected.

To be able to determine the cracks, the weld and the area around it were sprayed with white contrast colour, Byckotest 104. When a crack appeared a magnetic powder, Byckotest 103, were used to identify the spread.

7.4 Results

As stop criteria for the fatigue test, the amplitude was used. The test equipment was set to stop the test if the amplitude grow to large. This means that the crack length became different for each weld-end. The results were normalised to a specific crack-length (25 mm). This was done using the following assumptions:

- The material follows Paris Law according to

$$\frac{da}{dN} = C * \Delta K_I^n \quad (7.1)$$

with $C=2.33e-12$ mm/cycle and $n=3.1$.

- The crack is supposed to start from the weld-edge and pass trough the entire material. The stress intensity factor, K_I , is assumed according to edge-crack exposed for one-axial tensile stress [13].
- The whole stress-amplitude makes the crack grow.
- The stress is calculated as nominal bending-stress.

The corrected numbers of cycles are presented in Table 7.3. As seen not all weld-end resulted in a crack. Finally the achieved results are plotted in a Wöhler-diagram, figure 7.6.

Table 7.3. Corrected number of cycles for cracks in the origin-material.

<i>Beam nr.</i>	<i>Upper/Lower</i>	<i>Point</i>	<i>Original crack length</i>	<i>Nom. stress range</i>	<i>Number of cycles</i>
			[mm]	[MPa]	10^6
1	U	A	35	154.2	1.31
1	U	A	19	154.2	1.32
1	L	A	39	154.2	1.31
1	L	A	49	154.2	1.31
2	L	A	47	168.6	0.719
3	U	A	17	175.6	0.712
3	U	A	15	175.6	0.716
3	U	B	15	136.8	0.733
3	U	B	5	136.8	0.890
3	L	A	38	172.4	0.697
3	L	A	20	172.4	0.707
3	L	B	4	139.2	0.928
3	L	B	18	139.2	0.718

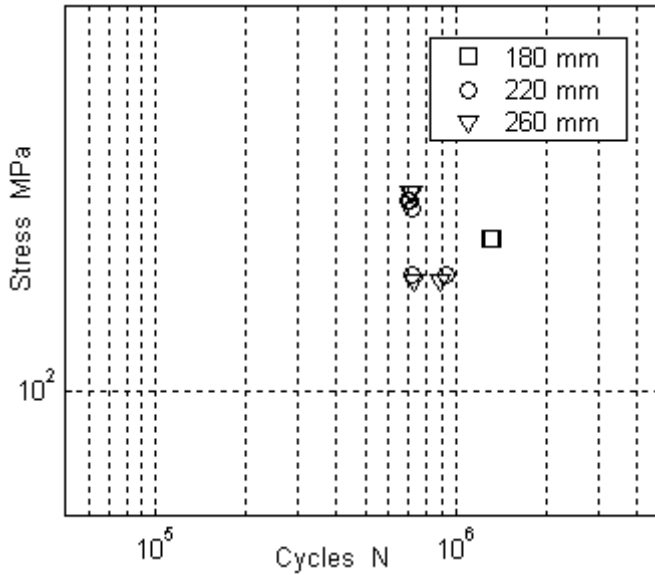


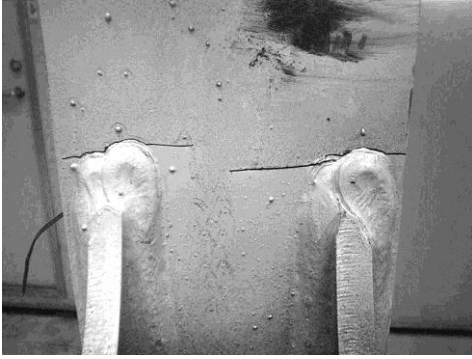
Figure 7.6. Wöhler diagram of the received results.

7.5 Hot-Spot Stress

The Hot spot stress, or geometrical stress, has been measured at two points. The stress was measured at point A on beam number 1, and at point B on beam number 3. The gauges were placed according to figure 3.1 and the stress at each point calculated according to equation 3.2. Finally the stress were calculated through linear interpolation towards the weld toe. In Table 7.4 the results from the three different ways of predicting the stress at the weld toe are compared.

Table 7.4. Comparison between different approaches.

	Hot Spot	Nominal	Volvo app.
	[MPa]	[MPa]	[MPa]
Beam 1			
Point A	98.0	77.1	82.5
Beam 3			
Point B	98.3	68.4	71.2



(a)



(b)

Figure 7.7. Crack propagation in beam (a) front view (b) side view.

8 Computer Program

To calculate the structural stress in a fast way a computer program in MATLAB was written. The program was developed for Windows NT Workstation and MATLAB version 4.2c. But it will work on other platforms and MATLAB versions as well.

The software was developed so that Volvo Construction Equipment could use it for further investigation of the method.

8.1 Input

To solve equation 4.9 for an arbitrary case the following data has to be available for the program:

- nodal co-ordinates
- element thickness
- local XYZ nodal forces
- local XYZ nodal moment of forces

All this information was exported from I-DEAS to a Universal file (UNV), that then was imported to MATLAB. The weld information, or more correct, the information from elements outside the weld toe, as well as the node numbers for the nodes located at the weld toe line were semi-manually saved in a separate file, a Node Element File (NEF).

8.2 Program Logic

The program consists of three parts. First it will import the UNV- and NEF files to a matrix file that MATLAB can read. Second it will sort out only the data that is needed for the stress calculation, with information from the NEF. The third step is to calculate element lengths, nodal forces perpendicular to the weld toe and nodal moment of forces parallel to the weld toe. Finally the element stresses along the weld line is calculated.

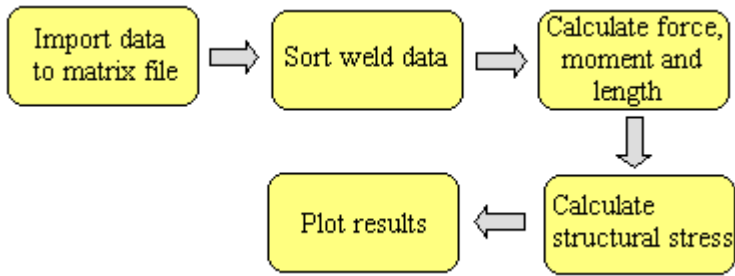


Figure 8.1. Main parts in the program code.

Nodes, elements and the path of the weld are plotted in a figure to make sure that the information in the NEF is correct. Figure 8.2 shows a closed weld that goes all around the attachment. The elements plotted in this figure are outside the weld toe, i.e. the elements that are encountered in the calculation. Different colours¹ are used in the plot to mark nodes, elements etc. The weld toe is in the program marked with a blue (black) line, element edges are green (gray), nodes red (gray star) and a black dot mark where the program starts the calculation. The direction of the calculation can be seen in the plot. The black dot indicates the start element and a green (gray) part of the otherwise blue (black) weldline indicates the last element of the calculation domain.

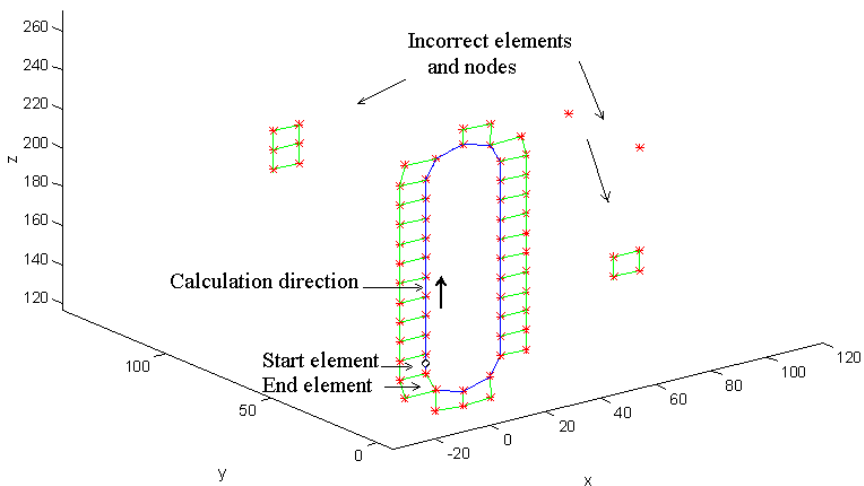


Figure 8.2. Plot intended to simplify the control of the data in the NEF.

¹ Since this report does not contain any coloured pictures explaining texts are put within brackets.

8.3 Output/Calculated Result

The calculated result or the output from the program is presented in a graph, figure 8.3, and the structural stress variation along the weld line is plotted in another graph, for example figure 4.8.

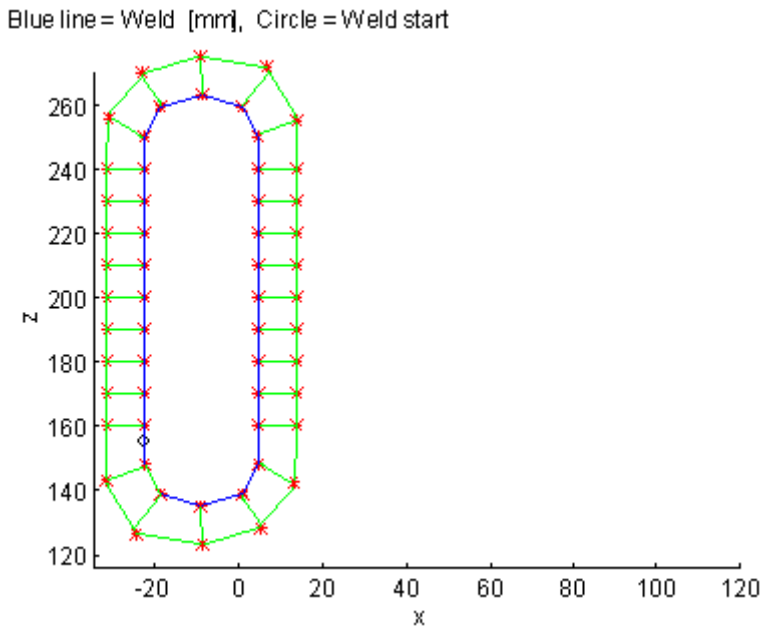


Figure 8.3. The FE-mesh around the weld.

9 Conclusions

A FE-based method for determining the structural stress perpendicular to the weld toe has been established and tested. Several different types of geometries have been used. The results show that there is no significant difference in stresses caused by bending moment or tensile force. This is in contrast to what Andréasson and Frodin [2] found in their thesis work. The results have been fitted into one curve in the SN-plot, figure 9.1. The slope of the curve was determined to -6.2.

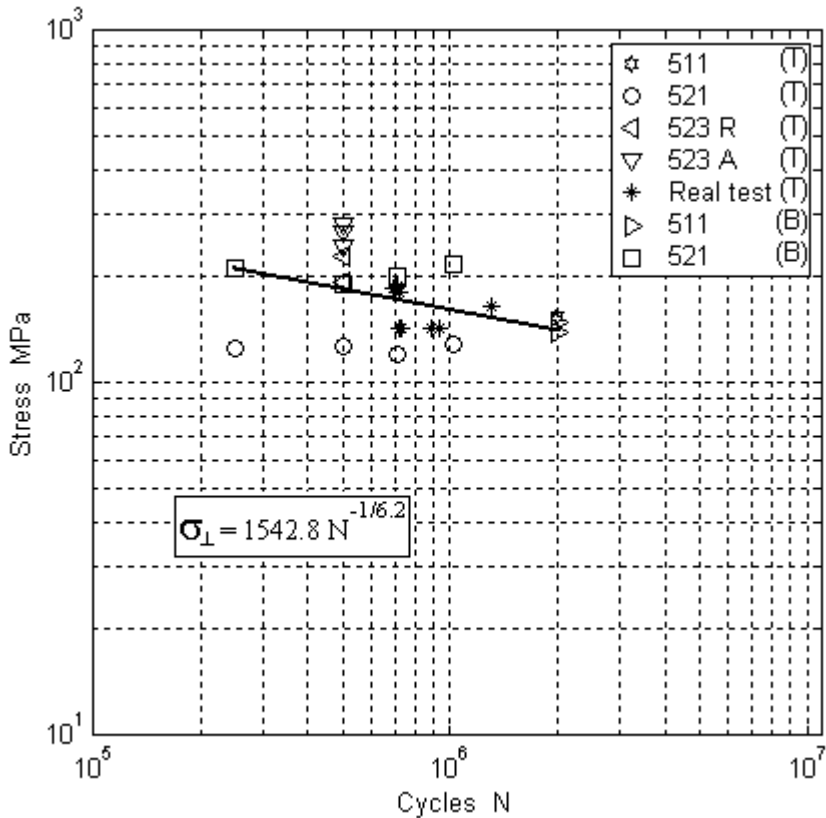


Figure 9.1. All results in one plot. (T) in the legend stands for tensile loaded and (B) for bending loaded.

A main idea was that the method should be more independent on the size of the mesh than an ordinary FE-solver. This appeared to be true. When using the Volvo approach the stress raises 6 % while decreasing the mesh-size from 10 to 2.5 mm. This should be compared with 26 % while doing the same in I-DEAS.

During the investigation of this thesis some other problems occurred as described in chapter 4.4. The Element Force in I-DEAS as well as GPFORCE in Nastran contained not only the load perpendicular to the weld-line but also the shear-force acting on the element-side, figure 9.2, so that e.g. the total force acting on node g_2 is

$$F_{g_2} = Q_2 + T_{xy} \tag{9.1}$$

For each FEM-program that will be used further on, this is a phenomenon that be must taken into consideration.

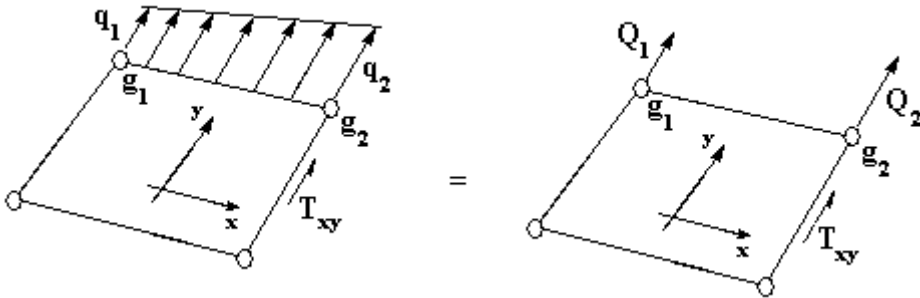


Figure 9.2. Forces acting on the element.

The last conclusion arises from an additional problem that appeared during the work. It is true that the mesh-size does not affect the results, but the appearance of the mesh does. Unlike previous works [1,2] the structures analysed were free-meshed. This mesh-procedure often generates elements that are distorted, although within the tolerances set in the program. Quite often a free-mesh also results in elements with only one node located at the weld toe. The method in its original edition is unable to handle this type of problems. Since this means that the method demands a great deal of manual work to be stable an expected advantage did not occur.

10 Further Work

During a project like this master thesis some questions are, because of limitations and lack of time, left without any answer. In this last chapter some of these questions are gathered and left open for further work.

The first question concerns the fact that a free mesh now and then generates elements with only one node located at the weld-line, e.g. as in figure 4.10. This means that equation 4.9 and 4.10 can not be solved. In this thesis making the mesh “semi-free” has solved the problem but this is not a practical method. Can the mesh be made in some other way or can the elements be included in the calculation using a separate equation?

Chapter 4.3 was devoted to investigate how a smooth corner should be modelled. It is not obvious that the chosen method is the right one. A corner can probably be modelled in many other ways.

In practice, the creation of a FE-model sometimes starts with a solid-model. Can the methodology be transferred onto this types of models and how?

11 References

1. Fayard J-L., Bignonnet A., Dang Van K., *Fatigue Design of Welded Thin Sheet Structures*, VTT symposium 156, Fatigue Design 1995, Vol II, VTT, Espoo, Finland, pp. 239-252.
2. Andréasson M. Frodin B. *Fatigue Life Prediction of MAG-welded Thin Sheat Structures*, Chalmers Tekniska Högskola, Göteborg, Report no. 97-138, Dept. 98270, 1997.
3. Hult J. *Bära Brista Fortsättningskurs i hållfasthetslära* 2nd edition, Almqvist & Wiksell, Stockholm, 1994.
4. Cook R., Malkus D., Plesha M., *Concepts and Applications of Finite Element Analysis*, John Wiley & Sons, USA, 1989. ISBN 0-471-84788-7.
5. A. Hobbacher, *Fatigue Design of Welded Joints and Components*, The International Institute of Weldein, England, 1996, ISBN 1-85573-315-3.
6. T. Dahlberg, *Teknisk hållfasthetslära*, Studentlitteratur, 1990, ISBN 91-44-31451-5.
7. E. Niemi, *Recommendations concerning stress determination for fatigue analysis of welded components*, International Institute of Welding, IIW, doc. XIII-1458-92/XV-797-92.
8. J. Solin, G. Marquis, A. Siljander, S. Sipilä, *Fatigue Design*, European Structural Integrity Society, ESIS, Publication 16, 1993, ISBN 0-85298-884-2.
9. M. Huther, J. Henry, *Recommendations for hot spot stress definition in welded joints*, IIW doc. XIII-1416-91.
10. Y. Murakami, *Stress Intensity Factors Handbook*, Pergamon Press, Oxford U.K., 1987.
11. Kleinlogel/Haselbach, *Rahmenformeln*, Verlag von Wilhelm Ernst & Sohn, 1974, ISBN 3-433-00660-1.
12. Volvo Koncernstandard, *Svetshandbok Dimensionering*, 1989.

13. B. Sundström, *Handbok och formelsamling i hållfasthetslära*, Institutionen för hållfasthetslära, KTH, 1998.